

DUAL-WIDEBAND BANDPASS FILTERS WITH EXTENDED STOPBAND BASED ON COUPLED-LINE AND COUPLED THREE-LINE RESONATORS

J.-T. Kuo^{1,*}, C.-Y. Fan², and S.-C. Tang³

¹Department of Electronic Engineering, Chang Gung University, Taoyuan, Taiwan

²Mediatek Corp., Hsinchu, Taiwan

³Institute of Communication Engineering, National Chiao Tung University, Hsinchu, Taiwan

Abstract—Coupled-line and coupled three-line resonators are proposed to design dual-wideband bandpass filters. Compared with the shorted and open stubs shunt at the same locations of the main line, in addition to saving the circuit area, these resonators provide alternative ways to the design of dual-wideband filters, with larger possible bandwidths and different frequency ratio of the two center passbands. The geometric parameters of the coupled-line and the coupled three-line structures are determined by deriving their equivalent circuits to a shunt open stub in parallel connection with a shunt shorted stub. To extend the upper stopband, a cross-shaped admittance inverter is devised to play the role of the 90-degree transmission line section at the center frequency and to create transmission zeros at the spurious passbands, so that the upper stopband of the filter can be extended. It is a quarter-wave section with two open stubs of unequal lengths shunt at its center. For demonstration, two dual-wideband bandpass filters operating at 900/1575 MHz and 900/2000 MHz are fabricated and measured. Measured results of the experimental circuits show good agreement with simulated responses.

1. INTRODUCTION

Bandpass filters are one of the key components in the RF front end of a microwave communication system. Design of single-band bandpass

Received 1 December 2011, Accepted 26 December 2011, Scheduled 9 January 2012

* Corresponding author: Jen-Tsai Kuo (jtkuo123@mail.cgu.edu.tw).

filters has been well documented in, e.g., [1]. Rapid advance of the modern wireless communication systems has created demands of multi-band active and passive microwave/RF devices. Design of dual-band filters at microwave frequencies is still challenging since it has to take into consideration many parameters, including center frequency, bandwidth, and/or passband functions at the two passbands. There have been many innovative dual-band bandpass filter designs [2–8]. In [2], compact miniaturized hairpin resonators are utilized in a 2×2 configuration to design two quasi-elliptic function passbands. Stepped-impedance resonator (SIR) is a versatile multi-resonance element suitable for multi-band purpose [3]. In [4], SIRs in parallel-coupled configuration are devised to synthesize a dual-band response. In [5], cascaded folded tri-section SIRs are used to design compact dual-band bandpass filters. In [6], dual-band filter are built by open-loop ring resonators incorporating with the electric and magnetic coupling structures. In [7], a dual feeding structure embedded uniform impedance resonator is used to design a dual-band bandpass filter. In addition, stub-loaded resonators are an alternative technique for such designs since the two center frequencies can be easily controlled by tuning length of the stub [8,9]. In [10], compact dual-band filters are developed based on the dual-resonance composite resonators by using integrated passive device technology on a glass substrate. The magnetic and electric mixed coupling in a high-density wiring transformer configuration generates multiple transmission zeros for enhancing passband isolation and stopband rejection. In [11], an extremely compact dual-band filter is designed with the meandered technology and fractal geometry. The skirt selectivity is attractive since two transmission zeros are created on both sides of the two passbands.

In [2,4–11], the center frequencies of the two passbands can be flexibly tuned; however, the design methods are rather suitable for narrow-band filters. It is well known that a shunt shorted stub can provide a wideband bandpass response whereas a shunt open circuit stub filter creates a bandstop response with a relatively small bandwidth [1]. Therefore, along the main transmission line, a shorted and an open stub connected in shunt at the same point will produce a wide passband with a narrow-band bandstop characteristic in the middle, or equivalently a dual-wideband bandpass response with good passband isolation [12]. In [13], SIRs are used to substitute both the shunt open- and short-stubs in order to have different bandwidths for the two designated passbands.

Stopband extension has been an important issue in filter design recently. Ideal bandpass filters have an infinite upper stopband.

Many effective techniques have been proposed and incorporated with the filter synthesis to achieve a wide upper rejection band [14–18]. For the parallel-coupled filters, higher order unwanted passbands occur at the multiples of the fundamental frequency. Suspended substrate structure [14] and the corrugated coupled-line in [15] are good techniques to make the even- and odd-mode phase velocities identical so that the spurious passband at the second harmonic can be suppressed. In [16], multi-spurious suppression is achieved by generating transmission zeros with over-coupled stages and the stopband can be extended to the fifth harmonic of the design frequency. In [17], SIRs are applied to push higher order resonances to much higher frequencies. With appropriate input/output tapping structure, extra transmission zeros are created to suppress the leading two higher order harmonics. In [18], dual-band bandpass filters are implemented by parallel coupled SIRs. The stopband performance is greatly improved by tuning the coupled lengths and the positions of the input/output transformers, which can provide multi-spurious suppression. To date, it has still been quite challenging to design dual-band bandpass filters equipped with a wide upper stopband, so that only few publications [19] can be found in open literature.

In this paper, coupled-line and coupled three-line resonators are proposed for design of dual-band bandpass filters with relatively wide bandwidths. A cross-shaped admittance inverter is also devised to extend the upper stopband. The extension relies on the creation of transmission zeros at the spurious passbands. The cross-shaped inverter consists of a transmission line section shunt with two open stubs at its middle. The lengths of the stubs are determined by the designated zero frequencies. Analysis formulas for the proposed inverter will be derived. This paper is organized as follows. Secs. 2 and 3 describe the resonance characteristics of coupled-line and coupled

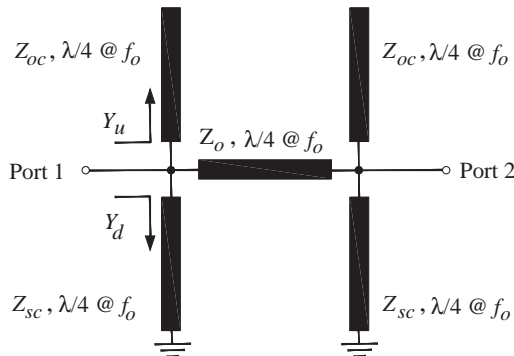


Figure 1. A second-order dual-wideband bandpass filter.

three-line resonators, respectively. Sec. 4 formulates the analysis of the proposed inverter for use to replace the conventional inverter and to create transmission zeros for multi-spurious suppression. Sec. 5 will compare the measured responses of two fabricated circuits with the simulation data, and Sec. 6 draws the conclusion.

2. CONVENTIONAL STRUCTURE AND COUPLED-LINE RESONATORS

Figure 1 depicts a second-order dual-band bandpass filter with parallel open-circuit and shorted stubs [12, 13]. The shorted stubs will generate a wideband bandpass filter, and at its center frequency the open stubs will create a bandstop filter with a smaller bandwidth. Their bandwidths are determined by the stub characteristic impedances. Obviously, both the bandpass and the bandstop filters share the same center frequency, denoted as f_o herein, since the Z_{oc} and the Z_{sc} stubs are commensurate. As a result, the circuit in Figure 1 possesses a dual-passband response with a rejection band in the middle. Let the center frequencies of the two passbands be f_1 and f_2 , respectively. It is known that both the above bandpass and bandstop filter responses are symmetric about f_o . Thus, the two bandwidths of the dual-passband response will be identical.

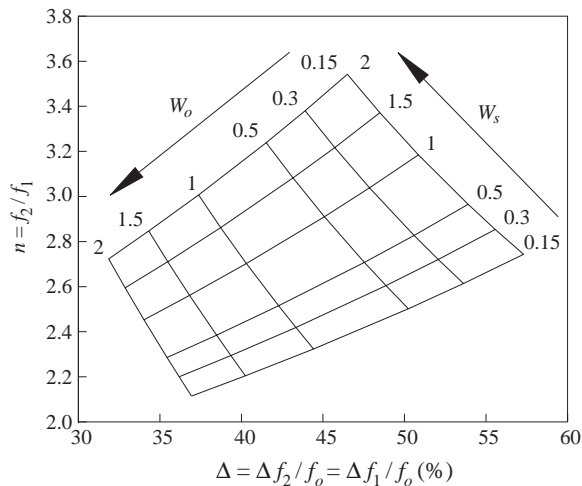


Figure 2. Frequency ratio and bandwidth design graph for the dual-band bandpass filter. Substrate: $\epsilon_r = 10.2$, thickness $d = 1.27$ mm. W_s and W_o denote the line widths of the short-circuited stubs and open-circuit stubs, respectively.

By using the microstrip technology, when the widths of the open stubs (W_o) and the shorted stubs (W_s) are given, the frequency ratio f_2/f_1 and bandwidth ($\Delta = \Delta f_1/f_o = \Delta f_2/f_o$) design graph can be established as shown in Figure 2, for a substrate with $\epsilon_r = 10.2$ and thickness of 1.27 mm. It is known that best resolution for practical microstrip fabrication is about 0.15 mm. From Figure 2, it can be observed that the frequency ratio is always larger than 2, and the fractional bandwidth is less than 60%.

In Figure 1, the input admittance looking to the two shunt stubs Y_{in} can be written as

$$Y_{in} = -jY_{sc} \cot \theta + jY_{oc} \tan \theta \tag{1}$$

where $Y_{sc} = Z_{sc}^{-1}$ and $Y_{oc} = Z_{oc}^{-1}$. Figure 3(a) shows the use of the coupled-line resonators. Obviously, the circuit area is reduced by around 50%, as compared with that in Figure 1. By treating the coupled-line as a four-port network, the 4×4 Y - or Z -matrix can be known [1]. By shorting two diagonal ports and open one of the two ports, the input admittance can be derived as

$$Y_{in} = -2j \frac{Y_{oe}Y_{oo}}{Y_{oe} + Y_{oo}} \cot \theta + \frac{j(Y_{oe} - Y_{oo})^2}{2(Y_{oe} + Y_{oo})} \tan \theta \tag{2}$$

where Y_{oe} and Y_{oo} are the even and odd mode characteristic admittances of the coupled-line. Comparing (2) with (1), we have

$$Y_{sc} = 2 \frac{Y_{oe}Y_{oo}}{Y_{oe} + Y_{oo}} \tag{3a}$$

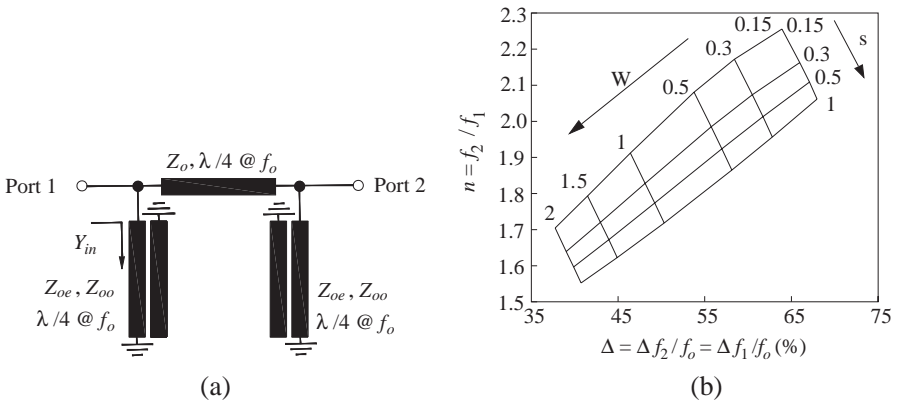


Figure 3. Dual-wideband bandpass filter with coupled-line resonators. (a) Schematic of the proposed coupled-line resonator structure. (b) Frequency ratio and bandwidth design graph. Substrate: $\epsilon_r = 10.2$, thickness $d = 1.27$ mm. W and s are respectively the line width and the gap size of the coupled-line.

$$Y_{oc} = \frac{1}{2} \frac{(Y_{oe} - Y_{oo})^2}{Y_{oe} + Y_{oo}} \quad (3b)$$

These two equations indicate that properly selecting the even- and odd-mode impedances $Z_{oe} = Y_{oe}^{-1}$ and $Z_{oo} = Y_{oo}^{-1}$ of the coupled-line, the dual-band bandpass filter in Figure 3(a) can be exactly equivalent to that in Figure 1. The fabrication resolution of the microstrip technology, however, will limit the realizable Z_{oe} and Z_{oo} , and hence the filter responses. Thus, the structure in Figure 3(a) will provide dual-band responses with different upper and lower limits of the frequency ratio $n = f_2/f_1$ and fractional bandwidth Δ . Figure 3(b) shows the frequency ratio and the bandwidth design graph of the dual-band bandpass filter with coupled-line resonators for a substrate of $\epsilon_r = 10.2$, $d = 1.27$ mm. It can be seen that the proposed structure greatly reduces the frequency ratio and increases circuit bandwidth.

3. COUPLED THREE-LINE RESONATORS

In this section, coupled three-line resonator shown in Figure 4(a) is proposed to realize dual-wideband bandpass filters in Figure 4(b). The line width and gap size of the symmetric coupled three-line structure are denoted as W and s , respectively. In [20], the eigenvoltage matrix for the three quasi-TEM modes can be written as

$$[M_v] = \begin{bmatrix} 1 & 1 & 1 \\ m_1 & 0 & -m_3 \\ 1 & -1 & 1 \end{bmatrix} \quad (4)$$

where m_1 and m_3 are positive real. As shown in (4), the modal voltages on the three lines for each mode are symmetric. For example, the eigenvoltages on the three lines for the first propagating mode are 1,

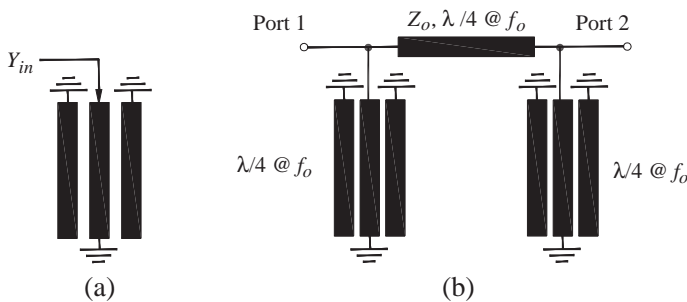


Figure 4. (a) Coupled three-line resonator. (b) Dual-wideband filter with coupled three-line resonators.

m_1 , and 1, indicating it is an even mode. Similarly, the second mode is an odd mode.

It can be shown [21] that the input admittance of the three-line resonator can be expressed as follows

$$Y_{in} = -j \frac{1}{(m_1^2 Z_{m1} + m_3^2 Z_{m3})} \cot \theta + j \frac{(m_1 Z_{m1} - m_3 Z_{m3})^2}{Z_{m1} Z_{m3} (m_1^2 Z_{m1} + m_3^2 Z_{m3}) (m_1 + m_3)^2} \tan \theta \quad (5)$$

where Z_{mi} ($i = 1, 2, 3$) represents the modal characteristic impedance of mode i . Comparing (5) with (1), the following relationship can be obtained:

$$Y_{sc} = \frac{1}{m_1^2 Z_{m1} + m_3^2 Z_{m3}} \quad (6a)$$

$$Y_{oc} = \frac{(m_1 Z_{m1} - m_3 Z_{m3})^2}{Z_{m1} Z_{m3} (m_1^2 Z_{m1} + m_3^2 Z_{m3}) (m_1 + m_3)^2} \quad (6b)$$

These results show that the coupled three-line resonator can also be exactly equivalent to the shunt connection of the open and shorted stubs. It is noted that when W and s are given, all the modal parameters for the three modes can be known [20]. Thus based on (6) the values of Y_{sc} and Y_{oc} can be nonlinear functions of W and s .

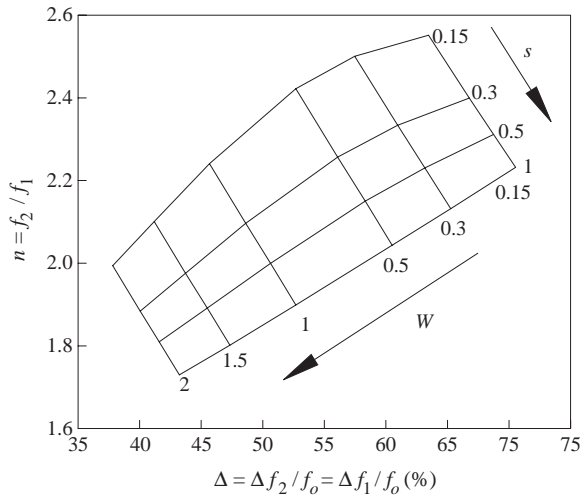


Figure 5. Frequency ratio and bandwidth design graph for coupled three-line resonators. Substrate: $\epsilon_r = 10.2$, thickness = 1.27 mm. W represents the line width and s denotes the gap size.

Figure 5 draws the frequency ratio and bandwidth design graph for of the dual-band bandpass filter with coupled three-line resonators. Table 1 compares the realizable frequency ratio n and bandwidths Δ by the three configurations.

4. CROSS-SHAPED ADMITTANCE INVERTER

All the stubs, coupled-line, and coupled three-line in Figures 1, 3 and 4 are quarter-wavelength long at f_o . Thus, a periodic bandpass response in the frequency axis can be expected, and the dual-wideband response will repeat itself at $3f_o, 5f_o, \dots$, etc. Figure 6 shows a typical frequency

Table 1. Realizable frequency ratio $n = f_2/f_1$ and fractional bandwidth Δ . Microstrip circuit substrate: $\epsilon_r = 10.2$, thickness = 1.27 mm.

Structure\Parameters	n_{\min}	n_{\max}	Δ_{\min} (%)	Δ_{\max} (%)
Shunt Open and Shorted Stubs (Figure 1)	2.14	3.54	31.9	57.3
Coupled-Line Resonator (Figure 3)	1.55	2.26	37.7	70.0
Coupled Three-Line Resonator (Figure 4)	1.73	2.55	38.2	75.0

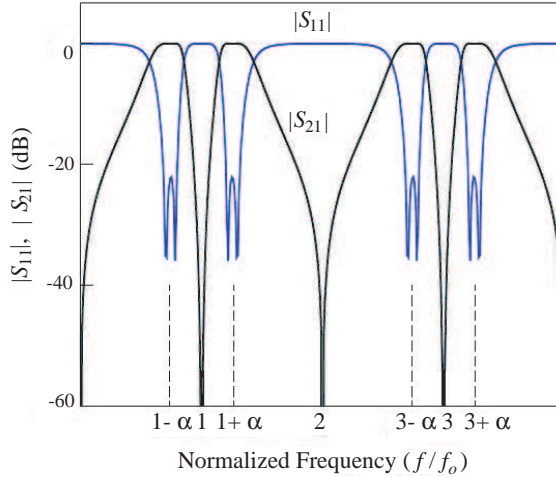


Figure 6. Typical frequency response of a dual-wideband bandpass filter. $Z_{sc} = 25 \Omega$, $Z_{oc} = 100 \Omega$, $Z_o = 50 \Omega$. $\theta = \pi/2$ at f_o .

response of a dual-band bandpass filter. It can be validated that for the structure in Figure 1 the two-port parameters can be calculated by

$$S_{11} = \frac{1 - y_e y_o}{(1 + y_e)(1 + y_o)} \tag{7a}$$

$$S_{21} = \frac{y_o - y_e}{(1 + y_e)(1 + y_o)} \tag{7b}$$

$$y_e = \frac{Y_{in}}{Y_o} + j \tan \frac{\theta}{2} \tag{7c}$$

$$y_o = \frac{Y_{in}}{Y_o} - j \cot \frac{\theta}{2} \tag{7d}$$

where $Y_o = Z_o^{-1}$ and Y_{in} is given in (1). The center frequencies of the two passbands can be written as follows:

$$f_1 = (1 - \alpha)f_o \tag{8a}$$

$$f_2 = (1 + \alpha)f_o \tag{8b}$$

where

$$\alpha = \frac{n - 1}{n + 1} \tag{8c}$$

$$n = f_2/f_1 \tag{8d}$$

Also, the center frequencies of the spurious passbands around $3f_o$ can be represented by

$$f'_1 = (3 - \alpha)f_o \tag{9a}$$

$$f'_2 = (3 + \alpha)f_o \tag{9b}$$

The targets to be suppressed for stopband extension are the spurious bands at f'_1 and f'_2 .

The main transmission line section between the stubs in Figures 1, 3 and 4 has an electrical length of 90 degrees. It plays as an admittance inverter in filter design. Obviously, when the operation

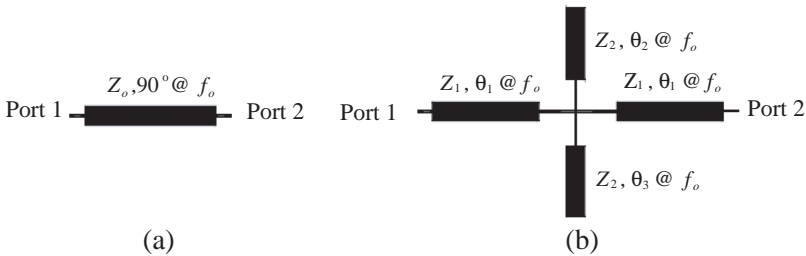


Figure 7. Admittance inverters. (a) Conventional admittance inverter. (b) Proposed cross-shaped admittance inverter.

frequency is increased to three times the center frequency, the electrical length of this section becomes 270° or -90° . It means the inverter also provides coupling between the two side resonators at $3f_o$. In this section, a cross-shaped admittance is proposed to substitute this inverter, and to produce two transmission zeros at around $3f_o$ to cancel the spurious passbands.

Figure 7(a) shows the conventional admittance inverter. The two-port Z -parameters of the inverter can be obtained through the even and odd analysis:

$$Z_{ino} = jZ_o \quad (10a)$$

$$Z_{ine} = -jZ_o \quad (10b)$$

Figure 7(b) shows the proposed cross-shaped inverter, consisting of a $2\theta_1$ -section with two open stubs shunt at its center. The main section has characteristic impedance Z_1 and the two open stubs have identical characteristic impedance Z_2 but different electrical lengths θ_2 and θ_3 . The input impedances of the proposed inverter with even and odd symmetric planes in the middle can be derived as

$$Z_{ino} = jZ_1 \tan \theta_1 \quad (11a)$$

$$Z_{ine} = -jZ_1 \frac{2Z_2 - Z_1 \tan \theta_1 (\tan \theta_2 + \tan \theta_3)}{Z_1 (\tan \theta_2 + \tan \theta_3) + 2Z_2 \tan \theta_1} \quad (11b)$$

Enforcing (11a) equal to (10a) and (11b) identical to (10b), we obtain

$$Z_1 = Z_o \cot \theta_1 \quad (12a)$$

$$Z_2 = Z_o \frac{\tan \theta_2 + \tan \theta_3}{1 - \tan^2 \theta_1} \quad (12b)$$

These equations indicate that if Z_1 and Z_2 are calculated based on given θ_1 , θ_2 and θ_3 , the cross-shaped inverter can be exactly equivalent to an ideal admittance inverter at the design frequency f_o . The values of θ_2 and θ_3 are chosen to generate two transmission zeros at f'_1 and f'_2 in (9) where the electrical lengths θ_2 and θ_3 are 90 degrees:

$$\theta_2 = 90^\circ / (3 - \alpha) \quad (13a)$$

$$\theta_3 = 90^\circ / (3 + \alpha) \quad (13b)$$

5. SIMULATION AND MEASUREMENT

Two experimental dual-wideband filters are fabricated and measured for validations. The circuits are fabricated on a substrate with $\epsilon_r = 10.2$ and thickness $h = 1.27$ mm. The simulation work is done by the software package IE3D [22]. Figure 8(a) shows the

layout of the first circuit with coupled-line resonators, and Figure 8(b) is the photograph of the measured circuit. It is designed to have $f_1 = 900$ MHz, $f_2 = 1575$ MHz, and fractional bandwidth $\Delta = 39\%$. The electrical lengths of the two shunt open-stubs of the cross-shaped inverter are $\theta_2 = 32.97^\circ$ and $\theta_3 = 27.52^\circ$ at f_o . Given $\theta_1 = 30^\circ$,

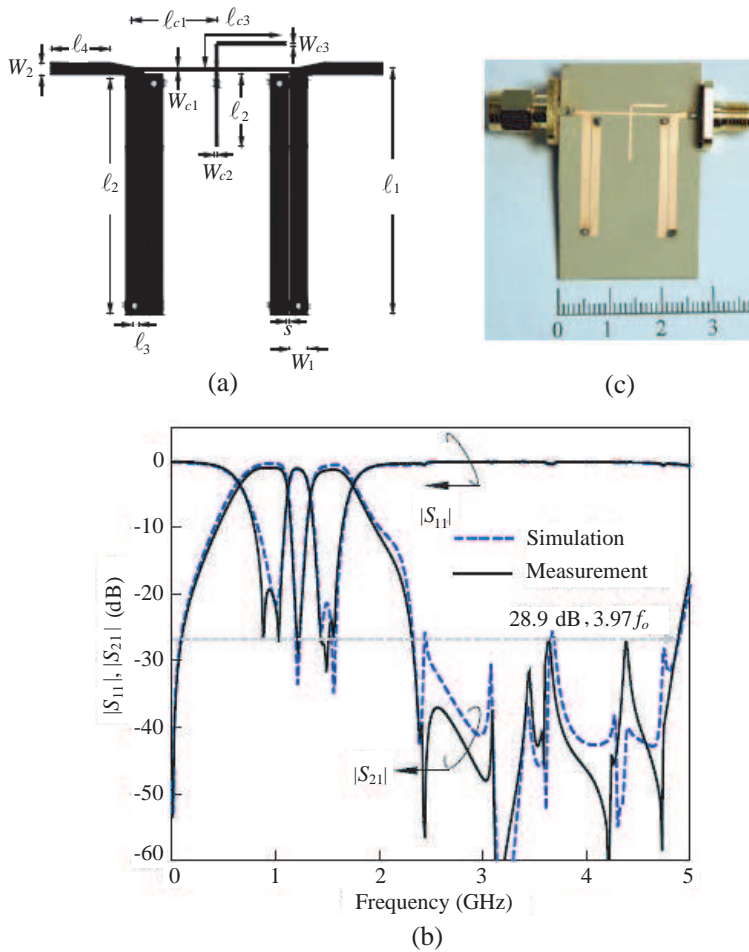


Figure 8. Performance of the dual-wideband bandpass filters with coupled-line resonators. (a) Circuit layout. (b) $|S_{11}|$ and $|S_{21}|$ responses. (c) Photograph of the experimental circuit. Geometric parameters: $l_1 = 23.89$ mm, $l_2 = 23.10$ mm, $l_3 = 0.65$ mm, $l_4 = 3.50$ mm, $W_1 = 1.76$ mm, $W_2 = 1.19$ mm, $s_1 = 0.15$ mm, $l_{c1} = 8.54$ mm, $l_{c2} = 9.32$ mm, $l_{c3} = 7.86$ mm, $W_{c1} = 0.54$ mm, $W_{c2} = 0.56$ mm, $W_{c3} = 0.56$ mm.

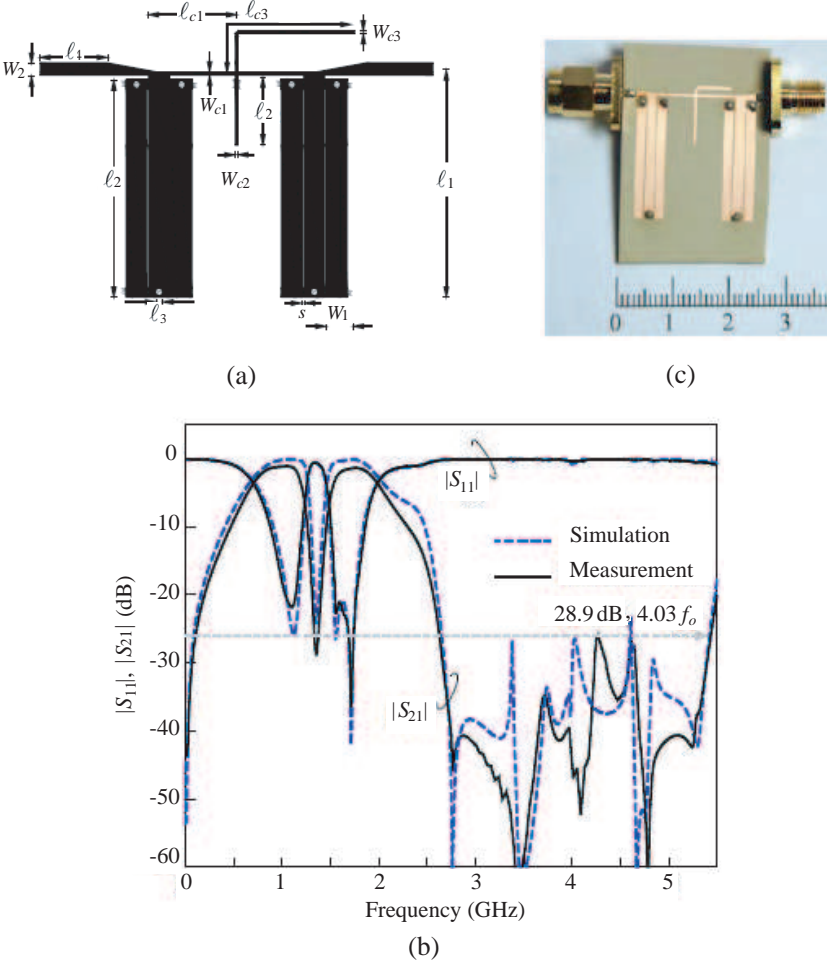


Figure 9. Performance of the dual-wideband bandpass filters with coupled three-line resonators. (a) Circuit layout. (b) Simulated and measured $|S_{11}|$ and $|S_{21}|$ responses. (c) Photograph of the experimental circuit. Geometric parameters: $l_1 = 22.09$ mm, $l_2 = 21.30$ mm, $l_3 = 0.65$ mm, $l_4 = 3.50$ mm, $W_1 = 1.97$ mm, $W_2 = 1.19$ mm, $s_1 = 0.15$ mm, $l_{c1} = 7.89$ mm, $l_{c2} = 8.73$ mm, $l_{c3} = 7.09$ mm, $W_{c1} = 0.52$ mm, $W_{c2} = 0.56$ mm, $W_{c3} = 0.56$ mm.

$Z_1 = 86.60 \Omega$ and $Z_2 = 87.72 \Omega$ are calculated by (12). Figure 8(c) compares the measured with the simulated responses. They show good agreement. The insertion losses at f_1 and f_2 are -0.987 dB and

-1.318 dB, respectively. The measured bandwidths are $\Delta_1 = 37.98\%$ and $\Delta_2 = 36.94\%$, showing small deviations from the design. The two transmission zeros created by the cross-shaped inverter are at 3.14 and 4.21 GHz. As shown in Figure 8(c), the spurious passbands near $3f_o$ are successfully suppressed. The upper stopband is extended up to 4.91 GHz ($3.97f_o$) for a reference insertion loss level of 28.9 dB.

Figure 9(a) shows the layout of the second experimental dual-wideband filter with the coupled three-line resonators, and Figure 9(b) depicts the photograph of the measured circuit. It is designed to have $f_1 = 900$ MHz, $f_2 = 1800$ MHz, and bandwidth $\Delta = 38\%$. The electrical lengths $\theta_2 = 33.71^\circ$ and $\theta_3 = 27.03^\circ$ are chosen. Let $\theta_1 = 30^\circ$, and $Z_1 = 86.60\Omega$ and $Z_2 = 88.29\Omega$ can be known from (12). Figure 9(c) draws the simulated and measured responses. The measured insertion losses at 900 and 1800 MHz are -1.38 dB and -1.49 dB, respectively. The two measured bandwidths are $\Delta_1 = 38.52\%$ and $\Delta_2 = 37.04\%$, showing negligible deviations from the design. The upper stopband is extended to 5.44 GHz ($4.03f_o$) for a reference insertion loss level of 25 dB, achieved by the transmission zeros generated by the cross-shaped inverter. The measured results match with the simulated responses quite well.

The circuit layout is developed based on the design graph in Figure 5, where effect of the cross-shaped admittance inverter on the coupling between the coupled three-line resonators is excluded. The differences between the designed and measured Δ_1 and Δ_2 are less than 0.5% and 1%, respectively. These are negligible deviations as compared with the designed 38%. This reflects the fact that the insertion of the cross-shaped admittance inverter has little influence on the design graphs in Figures 3 and 5.

6. CONCLUSION

Coupled-line and coupled three-line resonators are proposed and validated as good candidates for design of dual-wideband bandpass filters. These two resonators are used to play the role of an open stub and shorted stub shunt at the main transmission line. The fractional bandwidths and ratios of the two center frequencies realizable by these two types of resonator are compared with those of the design with shunt stubs. One of the advantages of the two proposed structures is that half of the area can be saved. A cross-shaped admittance inverters are proposed to create transmission zeros for upper stopband extension. The measured results not only confirm the analysis but also show good agreement with the simulation results obtained by commercial software package.

ACKNOWLEDGMENT

This work was supported in part by the National Science Council, Taiwan, under Grant NSC 98-2211-E-009-032-MY2 and Grant NSC 100-2221-E-182-059-MY2, and in part by the Chang Gung University, Taiwan, under Grant UERPD2A0021.

REFERENCES

1. Pozar, D. M., *Microwave Engineering*, 3rd Edition, Wiley, New York, 2005.
2. Kuo, J.-T. and H.-S. Cheng, "Design of quasi-elliptic function filters with a dual-passband response," *IEEE Microw. Wireless Compon. Lett.*, Vol. 14, No. 10, 472–474, Oct. 2004.
3. Chiou, Y.-C. and J.-T. Kuo, "Planar multiband bandpass filter with multimode stepped-impedance resonators," *Progress In Electromagnetics Research*, Vol. 114, 129–144, 2011.
4. Kuo, J.-T., T.-H. Yeh, and C.-C. Yeh, "Design of microstrip bandpass filters with a dual-passband response," *IEEE Trans. Microw. Theory Tech.*, Vol. 53, No. 4, 1331–1336, Apr. 2005.
5. Ma, D., Z.-Y. Xiao, L. Xiang, X. Wu, C. Huang, and X. Kou, "Compact dual-band bandpass filter using folded SIR with two stubs for WLAN," *Progress In Electromagnetics Research*, Vol. 117, 357–364, 2011.
6. Chen, C.-Y. and C.-Y. Hsu, "A simple and effective method for microstrip dual-band filters design," *IEEE Microw. Wireless Compon. Lett.*, Vol. 16, No. 5, 246–248, May 2006.
7. Yang, R.-Y., K. Hon, C.-Y. Hung, and C.-S. Ye, "Design of dual-band bandpass filters using a dual feeding structure and embedded uniform impedance resonators," *Progress In Electromagnetics Research*, Vol. 105, 93–102, 2010.
8. Zhang, X. Y., J.-X. Chen, Q. Xue, and S.-M. Li, "Dual-band bandpass filters using stub-loaded resonators," *IEEE Microw. Wireless Compon. Lett.*, Vol. 17, No. 8, 583–585, Aug. 2007.
9. Mondal, P. and M. K. Mandal, "Design of dual-band bandpass filters using stub-loaded open-loop resonators," *IEEE Trans. Microw. Theory Tech.*, Vol. 56, No. 1, 150–155, Jan. 2008.
10. Chen, C.-H., C.-S. Shih, T.-S. Horng, and S.-M. Wu, "Very miniature dual-band and dual-mode bandpass filter designs on an integrated passive device chip," *Progress In Electromagnetics Research*, Vol. 119, 461–476, 2011.

11. Chen, C.-Y. and C.-C. Lin, "The design and fabrication of a highly compact microstrip dual-band bandpass filter," *Progress In Electromagnetics Research*, Vol. 112, 299–307, 2011.
12. Yim, H.-Y. A. and K.-K. M. Cheng, "Novel dual-band planar resonator and admittance inverter for filter design and applications," *IEEE MTT-S Int. Microwave Symp. Dig.*, 2187–2190, Jun. 2005
13. Liu, A.-S., T.-Y. Huang, and R.-B. Wu, "A dual wideband filter design using frequency mapping and stepped-impedance resonators," *IEEE Trans. Microw. Theory Tech.*, Vol. 56, No. 12, 2921–2929, Dec. 2008.
14. Kuo, J.-T., M. Jiang, and H.-J. Chang, "Design of parallel-coupled microstrip filters with suppression of spurious resonances using substrate suspension," *IEEE Trans. Microwave Theory Tech.*, Vol. 52, No. 1, 83–89, Jan. 2004.
15. Kuo, J.-T., W.-H. Hsu, and W.-T. Huang, "Parallel-coupled microstrip filters with suppression of harmonic response," *IEEE Microw. Wireless Compon. Lett.*, Vol. 12, No. 10, 383–385, Oct. 2002.
16. Jiang, M., M.-H. Wu, and J.-T. Kuo, "Parallel-coupled microstrip filters with over-coupled stages for multispurious suppression," *IEEE MTT-S Int. Microwave Symp. Dig.*, 687–690, Jun. 2005.
17. Kuo, J.-T. and E. Shih, "Microstrip stepped-impedance resonator bandpass filter with an extended optimal rejection bandwidth," *IEEE Trans. Microw. Theory Tech.*, Vol. 51, No. 5, 1554–1559, May 2003.
18. Kuo, J.-T. and H.-P. Lin, "Dual-band bandpass filter with improved performance in extended upper rejection band," *IEEE Trans. Microw. Theory Tech.*, Vol. 57, No. 4, 824–829, Apr. 2009.
19. Mokhtaari, M., K. Rambabu, J. Bornemann, and S. Amari, "Advanced stepped-impedance dual-band filters with wide second stopbands," *Proc. Asia-Pacific Microw. Conf.*, 2285–2288, 2007.
20. Kuo, J.-T., "Accurate quasi-TEM spectral domain analysis of single and multiple coupled microstrip lines of arbitrary metallization thickness," *IEEE Trans. Microw. Theory Tech.*, Vol. 43, No. 8, 1881–1888, Aug. 1995.
21. Fan, C.-Y., "Dual-wideband bandpass filters with stopband extension," M.S. thesis, National Chiao Tung University, Hsinchu, Taiwan, Jun. 2010.
22. IE3D simulator, Zeland Software Inc., Jan. 2002.